

Modeling the Coevolutionary Dynamics in the *Lobaria pulmonaria* Lichen Symbiosis

Simon Carrignon^{1,2,*,*}, Aina Ollé-Vila^{2,3,*,*}, Salva Duran-Nebreda^{2,3,*,*}, and Julia N. Adams⁴

¹Barcelona Supercomputing Center, Carrer de Jordi Girona, 29-31, 08034 Barcelona, Spain.

²Institució Catalana per a la Recerca i Estudis Avançats-Complex Systems Lab, Universitat Pompeu Fabra, 08003 Barcelona, Spain.

³Institut de Biologia Evolutiva (CSIC-Universitat Pompeu Fabra), Passeig Marítim de la Barceloneta 37, 08003 Barcelona, Spain.

⁴Smithsonian Tropical Research Institute, P.O. Box 0843-03092, Panama, Republic of Panama

ABSTRACT

Lichenization is an evolutionarily and ecologically successful strategy for Ascomycete fungi, resulting in an estimated 18,000 lichen species. Although the nature of the lichen symbiosis is still widely debated, many sources agree that the lichen symbiosis represents an ecologically obligate mutualistic interaction whereby the net fitness of all partners is maximized. In order to elucidate the potential factors driving the evolution of the lichen symbiosis and the broader ecological and evolutionary interactions in the *Lobaria pulmonaria* model organism, an agent-based model was constructed using the ECHO framework. The ECHO tag system was used to model molecular recognition (receptors and physical embedding) between algal and fungal agents, two of the partners necessary to reconstitute the *L. pulmonaria* lichen symbiosis. We compared the simulations' results with a bipartite reconstruction of *L. pulmonaria* microsatellite data and our model reproduced some features of this data. Molecular data have shown that the mode of reproduction significantly affects within-population genetic structure of *L. pulmonaria*, most likely contributing to the modular structure of this population. Our results also show that the interaction type does not significantly alter network metrics (modularity and nestedness), showing that fungal-algal interactions ranging from parasitic to mutualistic can support a successful or a stable biological organism.

1 Introduction

Lichens are a hyperdiverse symbiotic group of organisms found in nearly every terrestrial ecosystem from the poles to the tropics and grow on diverse substrates, such as rocks (saxicolous) and the bark of trees (corticolous)¹. The partnership between a fungus (mycobiont) and a photobiont (cyanobacteria, algae, or both) allows the fungus to obtain carbohydrate-rich resources directly from their photosynthetic partner². In turn, the fungus protects the photobiont from desiccation and light intensity, leading to coevolution of the symbionts³ and adaptive radiation into new environments¹. The obligate symbionts are morphologically and physiologically integrated, resulting in the symbiotic structure known as the lichen thallus¹. The lichen symbiosis is an evolutionarily and ecologically successful strategy (>20% of fungi are lichenized), resulting in an estimated 18,000 lichen species^{1,4}. Although the nature of the lichen symbiosis is still widely debated, many sources agree that the lichen system represents an ecologically obligate mutualistic interaction whereby the net fitness of all partners is maximized^{4,5}.

The mode of reproduction strongly influences the genetic structure of lichen populations⁶, affecting dispersal and evolutionary rates. The majority of lichens can reproduce asexually and sexually¹. In the asexual mode of reproduction, mycobionts and photobionts are co-dispersed via fragmentation of the main thallus body or via specialized asexual propagules (isidia or soredia), resulting in genetically identical lichens (vertical transmission)^{1,6}. In the sexual mode of reproduction (horizontal transmission), the fungal spores (i.e. ascospores) are dispersed from specialized sexual structures known as ascomata. The ascospores must find a compatible algae, cyanobacterium, or both in order to reconstitute the lichen thallus (*relichenization*). The compatible photosynthetic partner can either be free-living⁷ or captured from another lichen⁸.

Lobaria pulmonaria is considered the best-studied lichen species worldwide from both an ecological and genetic point of view¹⁰. The foliose lichen is distributed throughout Europe and parts of North America and grows on the bark of several tree species in old-growth forests¹¹. *L. pulmonaria* is a lichen with a tripartite system consisting of an association among the green alga *Symbiochloris reticulata*¹², the cyanobacterium *Nostoc sp.*, and its main fungal host in Europe, *Lobaria*⁹. Recently, it has been shown that the mycobiont of *L. pulmonaria* is mostly dispersed together via asexual reproduction¹³, implicating long-term

*Authors contributed equally to this work. ‡Corresponding authors.

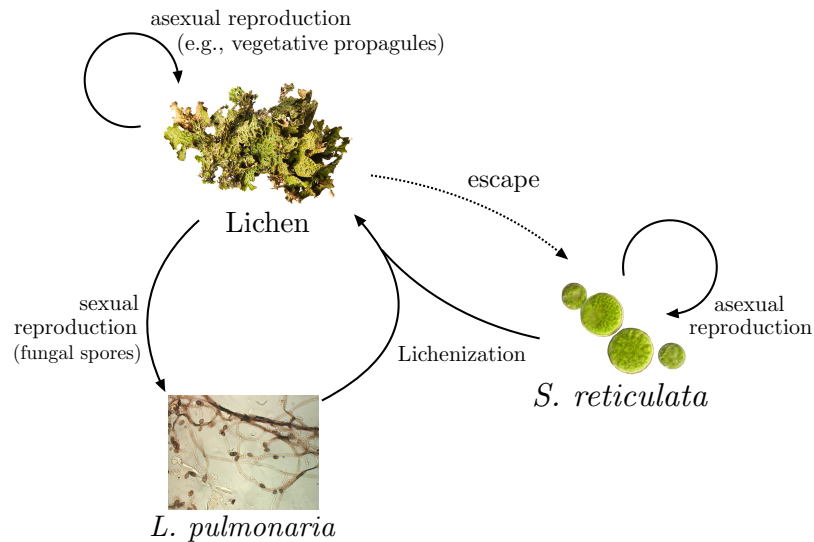


Figure 1. Life cycle of the *L. pulmonaria* system. Solid arrows represent sexual (via fungal spores) and asexual (e.g., vegetative propagules and thallus fragments) reproductive events, while the dotted arrow represents the process of the algae escaping the partnership via zoospores. Currently, little is known about the free-living status of the photobiont⁹. This figure summarizes the known (solid arrows) and inferred (dashed arrows) interactions between the agents of our model. Each process is governed by at least one parameter, some of which have been explored through a sensitivity analysis in our evolutionary algorithm.

interaction in the symbiosis^{6,13–156}. These lines of research have shown evidence of significant within-population genetic structure due to restricted gene flow and vertical photobiont transmission. However, recombination has been shown to occur a small percentage of the time⁶. The sexual mode of reproduction is suspected to play a central role at a larger evolutionary scale.

Recently, it has been shown that algal-sharing is ubiquitous throughout the Lobariaceae community. For instance, the same green algal photobiont genotype was shared among five co-occurring lichen species in the family of Lobariaceae⁹, providing evidence for photobiont exchange. These results support the photobiont-mediated guilds hypothesis, which occurs when photobionts are shared among different lichen species in a community within an evolutionary coherent structure¹⁶. This has the potential to occur during the sexual mode of reproduction when fungal spores are dispersed and capture photobionts in other fungal guilds⁸. This mechanism ensures survival of the photobiont and consequently relichenization of the entire fungal guild⁹. This relichenization process could be a successful strategy for genetic recombination, allowing lichens to access wider ecological niches by sharing photobionts among different lichens adapted to diverse local conditions. These loosely integrated functional units, whereby different partners can exchange resources and genetics materials, are good candidates to explain the evolutionary success of lichens. They allow different sub-components to evolve more or less independently, at different rates, and under different ecological niches, allowing the whole community to adapt to a wider range of changing environmental conditions.

Empirically studying the evolutionary dynamics of these assemblages is a difficult task because it involves a broad range of heterogeneous entities that coevolve and interact ecologically at various spatio-temporal scales. Experimental work is also difficult because lichens are fragile biological entities extremely dependent on their local environmental conditions, which are complex and difficult to reproduce in the laboratory¹. One solution to overcome these obstacles is to use computer simulations, which allows the study of a wide range of parameters involving a massive number of heterogeneous entities. The goals of this study were to 1) model the coevolutionary dynamics between the algal and fungal partners within a lichen under various conditions in a continuous evolutionary algorithm and to 2) compare the bipartite network structure from simulations to microsatellite data⁶ of the *L. pulmonaria* lichen system to better understand the local processes of dispersion and reproduction. In order to elucidate the potential factors driving the evolution of the lichen symbiosis and to better understand broader ecological and evolutionary interactions, this study investigated whether a continuous evolutionary algorithm could reproduce general features of empirical data from 62 populations of *L. pulmonaria* across Europe, America, Asia, and Africa.

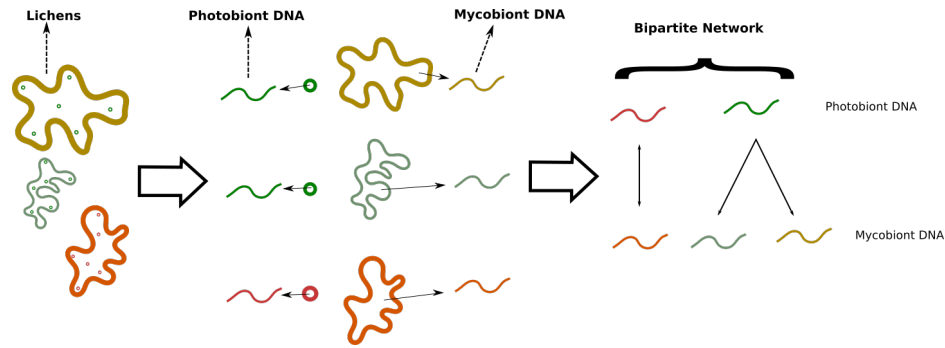


Figure 2. Construction of a bipartite network of symbionts from sequencing data. We separated the microsatellite data from the photobiont (algae) and the mycobiont (fungi), and constructed a bipartite network with these two lists. One node corresponds to a unique photobiont multilocus genotype (MLG_A) and the other node corresponds to a unique mycobiont multilocus genotype (MLG_F). Nodes were connected as edges when there was a direct observation of a particular pair (A_n, F_n) and when nodes were close in sequence space (see section 2.3).

2 Materials and Methods

2.1 Data set

We used an available data set from Dal Grande et al.⁶, which consists of 62 populations of *L. pulmonaria* (1960 thalli in total) in forests throughout Europe, America, Asia and Africa. These populations were genotyped at eight fungal-specific (LPu03, LPu09, LPu15, LPu23, LPu24, LPu25, LPu28) and seven algal-specific microsatellite markers (LPh1-LPh7). This approach allows for the reliable identification of lichen thalli with identical fungal and algal multilocus genotypes and allows for fine-scale marker resolution. This is critical for identifying genetically distinct individuals in populations of the same species⁶.

2.2 ECHO model

In order to model the coevolutionary dynamics between both partners in a lichen and the process of lichenization we devised some modifications to the ECHO model as defined by John Holland¹⁷ (code in Netlogo available upon request). The ECHO model typically consists of a collection of entities living in a bidimensional spatial domain (Ω), which can move around -typically as random walkers- and interact with one another and with their environment. The interactions among agents can be used to model different kinds of processes -such as mating-, and are driven by locality as well as agent-specific properties, namely the agents' genotypes. The ECHO model is also a continuous genetic algorithm¹⁸; upon reproduction old genotypes are copied with slight mutations, giving rise to quantifiable evolutionary dynamics.

In this work, we used the tag system of ECHO¹⁷ to model the molecular recognition -receptors and physical embedding- between algae and fungi necessary to create a new lichen. We considered two different lichenization functions based on similarity among the interacting agents' genotypes: sigmoid (hill function with $n = 2$) and Michaelis-Menten (saturation dynamics). Additionally, other ecologically relevant features such as dispersal rates were included in the model. Simulations were carried out assuming two types of ecological relations between the algae and fungi: parasitism (only one type of agent benefits from the partnership) and mutualism (both agents benefit).

Finally, the last free parameter explored within the system were the ratios of sexual to asexual reproduction. All possible combinations of ecological interactions and lichenization functions were expanded with varying rates of sexual reproduction (10^{-2} , 5×10^{-2} , 10^{-1} , 5×10^{-1} , 10^0 times the intrinsic asexual reproduction rates). For each condition in the parameter set, the simulations were run for 10^5 iterations of the algorithm, and the position in Ω as well as the genotypes of both the algae and the fungi of every single lichen were recorded. The bipartite networks were built from the interactions between algae and fungi forming a lichen at particular time points. Results reported here stem from a 5 replicate average.

2.3 Reconstruction of bipartite networks

We separated the lists of algal and fungal microsatellite data⁶ to create a bipartite network of the relationships among symbionts. For each algae A_n , in symbiosis with a fungus F_n , we looked for the existence of another fungus F_m in symbiosis with another algae A_m "similar" to A_n , and created a link between A_n and F_m . As a preliminary test, we considered two symbionts as "similar" when they shared the same microsatellites, that is, they represent the same "Multilocus Genotype" (MLG). Therefore, we assumed that genetically similar symbionts have a higher probability of sharing the same ancestor. This method, illustrated in Fig. 2, allowed us to create a bipartite network of interactions among all the unique MLG of the algae (MLG_A) with all the unique MLG of the fungi (MLG_F). We generated this graph for each lichen population in the data set⁶ (one example of the

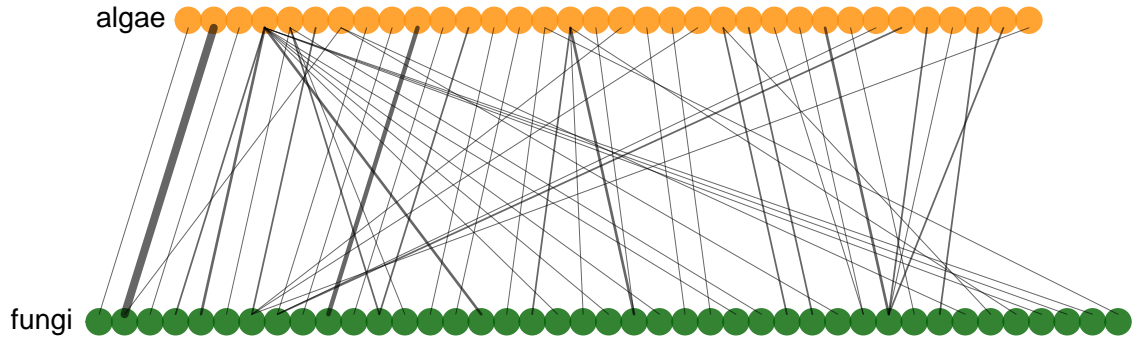


Figure 3. Bipartite network of Algae-Fungi Multilocus Genotypes (MLG) interactions from all lichens of the population #29 in the Dal Grande *et al.* (2012) dataset⁶. Each node represents one unique *MLG*, defined by a unique list of microsatellites. Yellow nodes represent the Algae's *MLG* and green nodes represent the Fungus' *MLG*. A link between two nodes indicates that two *MLG*'s were in symbiosis in at least one lichen. Edge weight (width and the darkness of the link) is directly proportional to the number of times the two *MLG*s have been found in symbiosis together.

resulting network is shown in Fig. 3) and performed the same analysis on this data set and the simulations' output (obtained from the model detailed in Section 2.2). In the latter case, symbionts' *tags* were used to group individuals sharing the same ancestor. In the data set by Dal Grande *et al.* (2012)⁶, each lichen population contained approximately 32 lichens. At the end of each simulation, the output contained approximately 1000 lichens (depending on the rate of reproduction and other factors). In order to effectively compare the networks extracted from the Dal Grande *et al.* (2012) data set⁶ and the ones built from the results of our simulations, we performed a scaling on the latter. We normalized the simulations' data set by dividing the output lattice of the model into roughly 60 similar sub-populations (in terms of surface size, see Fig. 4). This led to sub-populations with between 5 and 90 lichen samples. We constructed two sets of networks: one where all the lichens from one simulation were considered as a unique population, the other where the simulation output was considered as 60 different populations. Given the population size generated by the simulation described in section 2.2, we obtained 1500 networks in the first set and 90000 in the second one. In the following sections, we used both sets of networks and compared the results retrieved for each data set.

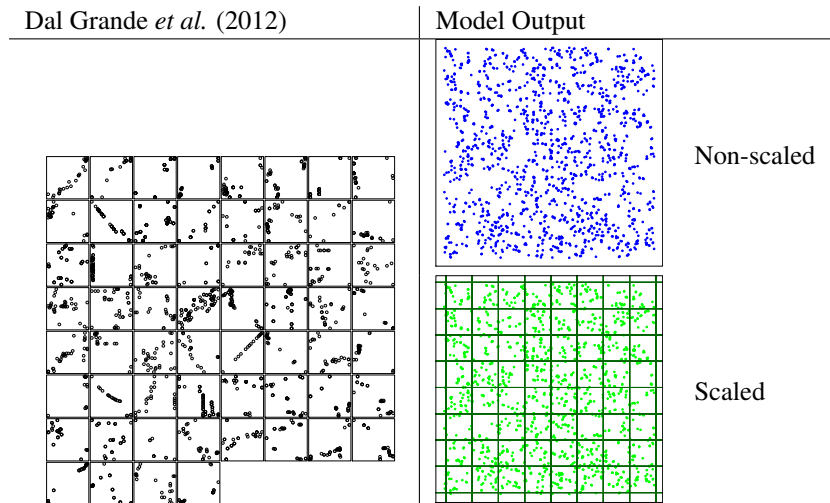


Figure 4. Rescaling of the data in the present study. The left panel shows the spatial locations of lichen populations from Dal Grande *et al.* (2012)⁶ side by side. The right panels (non-scaled and scaled) show the spatial locations of lichens after a typical simulation of our model. The bottom right panel shows the artificial separation we added in order to recreate roughly 60 sub-populations. This number is closer to the one found in the original data set.

2.4 Network metrics

2.4.1 Modularity

A network is said to have community structure if the nodes of the network can be easily grouped into (potentially overlapping) sets of nodes such that each set of nodes is densely connected internally. Maximize modularity is a way to detect community structure in networks, as it measures the quality of a particular division of a network into communities.

We used the leading eigenvector method proposed by Newman and Girvan¹⁹, which was later adapted for bipartite networks by Barber²⁰ to measure modularity in our data sets. The method defined by Barber detects communities including both types of nodes, as opposed to the measure proposed by Larremore *et al.* 2014²¹, where communities are formed by nodes of the same type. As we are interested in finding communities at the lichen symbiosis level, we used the method described by Barber. The goal of this method is to maximize the following equation,

$$Q = \frac{1}{|E|} \sum_{ij} (B_{ij} - \frac{k_i d_j}{|E|} \delta(g_i, h_j)) \quad (1)$$

where $(B_{ij} - \frac{k_i d_j}{|E|})$ is the so-called modularity matrix (see Barber 2007²⁰ for details). With this method, putative modules and the modularity metric within the network were obtained. The software package Bimat²² was used to compute these metrics.

2.4.2 Realised Modularity

Realised modularity is simply defined as the ratio of interactions established between members of the same modules (L_i) versus members of different modules (L_o)²³ as follows,

$$Q_r = \frac{L_i}{L_o} \quad (2)$$

The software package Bimat²² was also used to compute this metric.

2.4.3 Nestedness

Nestedness is a concept borrowed from island biogeography²⁴, which describes the extent to which interactions form ordered subsets of each other²⁵. In a perfectly nested matrix, each species would interact only with proper subsets of those species interacting with the more generalist species²⁶. Although there are several proposed metrics for quantifying this property, we used the NODF nestedness metric, which is based on the extent to which a network exhibits decreasing fill and paired overlap. This metric is normalized for matrix size (i.e. takes values between 0 and 1), allowing for comparison of networks of different sizes. A value of 0 indicates the lack of decreasing fill and paired overlap. A value of 1 corresponds to a perfectly nested matrix. The software package BiMAT²² was used to compute the nestedness of the networks generated from the data set and the model simulations. The equations used are shown as follows,

$$N_{NODF} = \frac{\sum_{ij} M_{ij}^{row} + \sum_{ij} M_{ij}^{col}}{[\frac{m(m-1)}{2}] + [\frac{n(n-1)}{2}]} \quad (3)$$

$$M_{ij}^{row} = \begin{cases} 0 & \text{if } k_i \leq k_j \\ n_{ij}/\min(k_i, k_j) & \text{otherwise} \end{cases} \quad (4)$$

where m and n are the number of rows and columns, respectively and k_i and k_j are the number of interactions in rows i and j . In turn, n_{ij} is the number of shared interactions between rows i and j . NODF measures the nestedness of the interaction matrix across rows by assigning a value M_{ij}^{row} to each pair i, j of rows. Positive contributions to NODF require pairs of rows to exhibit decreasing fill, which is satisfied when $k_i > k_j$ -meaning that the degree of node i is bigger than that of node j . A similar term M_{ij}^{col} is used to compute column contributions. The total nestedness is the sum of column and row contributions²².

3 Results

3.1 Parasitism versus Mutualism

Parasitic and mutualistic interactions among symbionts show very similar results regarding modularity (Q_b), number of modules, realised modularity (Q_r) and nestedness (Table 1). A few values were significantly different, which is most likely due to the high quantity of networks compared. Table 1 shows the mean properties of the networks collected at 60 000 time iterations for the different configurations. Equality between mutualistic and parasitic relationships holds for the entire simulation time (data not shown).

SRP (%)	Number of Module			Qr ratio			Modularity (Qb)			Nestedness		
	P	M	pval	P	M	pval	P	M	pval	P	M	pval
1	169.43	159.39	0.01	0.83	0.83	0.72	0.89	0.89	0.82	NA	NA	NA
5	75.03	74.19	0.55	0.38	0.39	0.09	0.65	0.65	0.19	NA	NA	NA
10	53.51	54.40	0.49	0.30	0.29	0.49	0.60	0.60	0.42	< 0.01	< 0.01	0.83
50	35.77	35.76	0.99	0.25	0.24	0.02	0.57	0.56	< 0.01	< 0.01	< 0.01	0.12
100	34.16	34.20	0.96	0.25	0.24	< 0.001	0.57	0.56	< 0.001	< 0.01	< 0.01	0.09

Table 1. Comparison of different network properties for simulations with parasitic (P) and mutualistic (M) interactions with different Sexual Rate Percentages (SRP). Each value represents the mean properties of the networks extracted from the output of the simulation at the 60000th iteration. The same results hold for every iteration of the simulations (data not shown).

3.2 Impact of sexual reproduction on Fungal-Algal bipartite network modularity

3.2.1 Temporal dynamics

In Fig. 5 we observe the evolution over time of modularity and the number of modules in bipartite networks retrieved from simulations with different sexual reproduction percentages (SRP i.e. the rate of sexual reproduction, see section 2.2). Evolution of modularity and the number of modules across simulation time varied according to the presence or absence of grid scaling (see Section 2.3). Moreover, the SRP parameter played a role regarding the number of modules and the modularity measure. However, this effect seems to be far more visible at a larger scale (non-scaled grid).

In the scaled grid, an increase both in the number of modules and modularity occurs across simulation time. Hence, we observe how the lichen population is getting a more modular structure as it evolves in time. The fact that we observe an increase either in modularity and the number of modules in the scaled grid allows to confirm that the population has a modular structure occurring locally. An amplification phenomena can be detected here, where species closely related genetically (which will, due to the dynamics of the model entities, be closely located in space) will tend to have higher likelihood of interaction with also closely related symbionts, forming modules. At the beginning of the simulation this phenomena cannot be observed, as tags are distributed randomly across the lattice and this population structure hasn't been formed yet.

In the other hand, we observe how the modularity measure Q_b decreases slightly at the beginning of the simulations for the non-scaled grid, while the number of modules increases across simulation time. This can be explained due to the dynamics of the entities taking part in the simulation. Initially, as the tags are distributed randomly across the lattice, the number of interactions is relatively low, as algae-fungal compatible tags don't need to be colocalized in space. Therefore, having a poor number of connections, the number of modules will be low. However, these modules will with high likelihood be very independent between them, with few intermodule connections. This would provoke the high value of modularity at the very beginning of the simulation we observe. This modularity measure decreases when the interactions number increase and more intermodule connections are established.

The same figure shows the influence of SRP in the temporal dynamics of these measures. The increase or decrease in the SRP does not seem to deeply affect the evolution of the number of modules or modularity at a local scale (scaled grid); however, this is not the case of the population at a large scale (non-scaled grid). In the latter case, a small increase in the rate of sexual reproduction is enough to drastically reduce the number of modules and the modularity measure observed in the bipartite network. The number of modules is roughly divided by 3 when increasing the percentage of sexual reproduction from 1% to 5% (from a mean of 150 modules per network to a mean of 60 modules), while the modularity decreased from 90% to 65% with the same increase.

The statistical significance of differences observed in temporal plots when simulations reach equilibrium can be seen in Figure 6.

3.2.2 Comparison with real data

To validate our model, we compared the number of modules and the modularity metric observed in the simulations after 60000 iterations (when simulations reached equilibrium, see Fig. 5) with empirical data from the Dal Grande *et al.* (2012) data set⁶. We compared values in Fig. 6 of those network metrics to the ones in the network built from the Dal Grande *et al.* (2012) data set. As was done for the temporal analysis, we compared the sets of networks (see section 2.4) built from the entire population (non-scaled, in blue) and the ones built from sub-populations (scaled, in green).

For both network metrics (modularity and number of modules) results were closer to the empirical data when the networks were scaled. This is expected, as the scaled populations were comparable in size to the populations in the original data set. For the scaled set of networks, the sexual rate of reproduction did not have a major effect on the network metrics values. Regardless of the SRP value (ranging from 1% to 100%), the networks obtained from the scaled model were able to more reliably reproduce

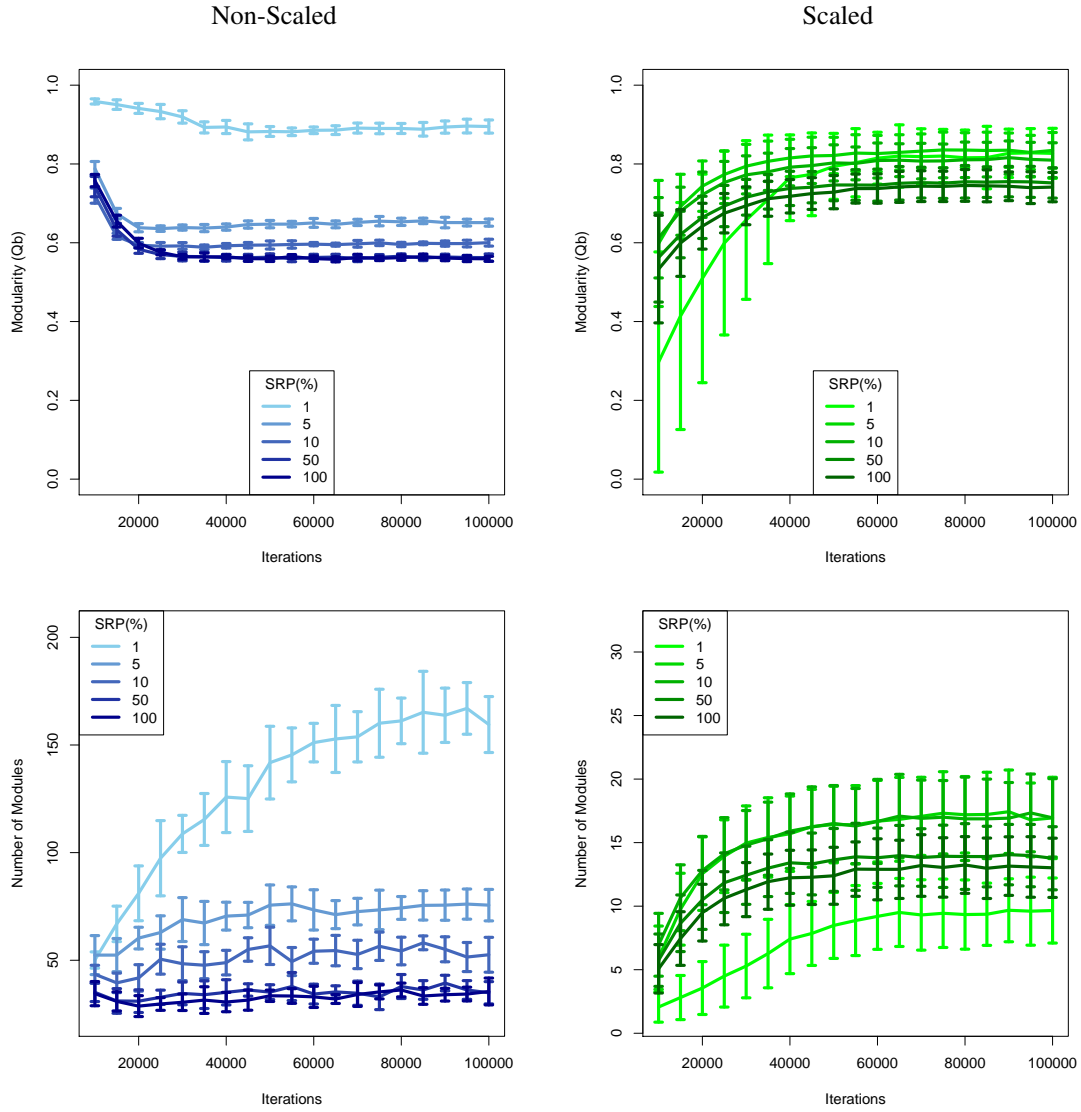


Figure 5. Evolution over time of modularity Q_b (top) and the number of modules (bottom) in bipartite networks reconstructed from simulations with different rates of Sexual Reproduction Percentage (SRP). The blue curves (left) correspond to the properties of networks that build upon the whole simulation, while the green curves (right) correspond to the properties of networks that build upon the scaled sub-population.

the modular structure of the empirical dataset than the non-scaled networks. However, the lowest SRP rate (10^{-2} times the intrinsic asexual reproduction rate) matches more closely the results from the empirical data in terms of both modularity and number of modules. Interestingly, the SRP do show a much major impact regarding the modular structure of the non-scaled data.

4 Discussion

In this work, we proposed an ECHO-like model encompassing the basic interactions between fungi and algae in order to better understand the evolutionary dynamics of lichenization. Specifically, we explored several parameters of the model that are typically regarded as influential in coevolutionary systems in general and *L. pulmonaria* in particular, such as the type of ecological interaction (*i.e.* parasitism or mutualism) and the presence of sexual reproduction used conjointly with propagule formation or other modes of asexual reproduction.

As previously stated, the nature of the ecological interaction between the two partners appears to have little relevance in deciding the general features of the reconstructed genotype-genotype bipartite network, both in terms of nestedness and

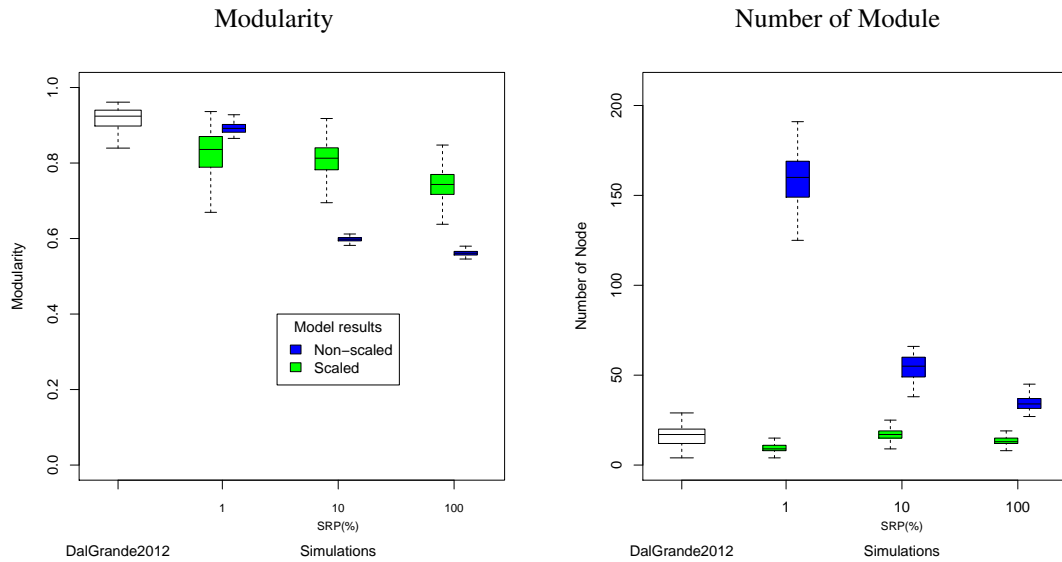


Figure 6. Comparison of the modularity (left) and of the number of modules (right) in bipartite networks observed in the data set of Dal Grande *et al.* (2012)⁶ with the networks at the end of simulations for increasing sexual reproduction rate. The blue boxes correspond to the properties of the networks built upon the whole simulation (non-scaled), while the green boxes correspond to the properties of networks built upon the scaled sub-population.

modularity measures. These results potentially stand in stark contrast to a body of literature that traditionally equates mutualistic bipartite networks to nested structures²⁵, typically through increased biodiversity²⁷ and stability²⁸ of the ecosystem.

On the other hand, as initially explored by Dal Grande *et al.* (2012)⁶, sexual reproduction does appear to have an impact on the population structure of lichens. In particular, we observed that it can drastically change the dynamics as well as the endpoint values of some network metrics under small changes in the incidences of sexual reproduction. Consistent with previous studies⁶ using spatial and genetic information, we have found that lower values (in-model value of $10^{-2} \times$ asexual reproduction rates) are the most consistent with the experimental data.

The rationale behind low rates of sexual reproduction are still poorly understood. A common hypothesis argues that sexual reproduction could be central to the persistence and evolution of the "photobiont-mediated guilds"^{9,16}. Our study at two different scales suggests that, although the role of sexual reproduction does not have a huge impact on the interaction properties at the local level (Fig. 5, left), it does have an impact on the temporal dynamics of the bipartite system at a large scale (Fig. 5, right). Our results are consistent with the photobiont-mediated guilds hypothesis, whereby sexual reproduction via algal-sharing among fungal guilds has an important role at a larger evolutionary scale.

Switching smoothly from a local to a global scale on real networks is a difficult task, as it is often hard to know how to sample both scales meaningfully. Given the fact that our model can successfully reproduce well-known local properties (see Fig. 6), we also think it is a good candidate to study the photobiont-mediated guilds -complex entities where different species co-evolve symbiotically and asymbiotically at different tempos and scales.

In nature, a lichen organism faces multiple evolutionary pressures due to environmental conditions from the local environment (e.g., temperature, precipitation, and altitude), stochastic and deterministic environmental factors, and biotic interactions. Therefore, this model can be expanded in several meaningful ways. First, we confined ourselves to model an essentially static two species system. However, in order to study multi-species systems such as photobiont-mediated guilds, the model should be scaled up to larger spatial areas. In doing so, reproduction, mutation rates, and types of ecological interactions can evolve, leading to the emergence of speciation events. In addition, scaling the model to larger spatial areas is important to understand the role that biogeography plays in the diversification of mycobionts and photobionts. For the sake of simplicity, we did not introduce any anisotropy (humidity or available sunlight for instance) or terrain complexity²⁴. However, in an attempt to understand networks involving species interacting at different spatial scales, diverse local environmental conditions should be included, as it is expected to play an important role in the evolutionary ecology of lichen communities. The model also does not include biotic interactions such as predation by arthropods and vertebrates and competition for space and resources by other lichens, bryophytes and fungi. In the future, spatio-temporal variability of these species interactions should be included, as they are also expected to play an important role in the evolutionary dynamics of lichen populations.

In conclusion, our work successfully modeled simple dynamics at different scales of the *L. pulmonaria* system, in

which the coevolutionary dynamics are still poorly understood. Therefore, we not only expect this work to strengthen the current knowledge of the coevolutionary dynamics in the *L. pulmonaria* system, but also to give insight into a more general understanding of coevolutionary systems whereby a set of species interact and form loosely defined emergent levels of biological organization.

Acknowledgements

This work was initiated at the 2016 Complex Systems Summer School (CSSS) at the Sante Fe Institute (SFI). The authors would like to thank all SFI resident faculty members, SFI external faculty members, SFI Omidyar Postdoctoral Fellows, and 2016 CSSS course participants for productive discussions as well as SFI staff during the 2016 CSSS. The authors would also like to thank Dr. Christoph Scheidegger for access to multiple data sets and Dr. Francesco Dal Grande for providing detailed knowledge of the *L. pulmonaria* system.

References

1. Nash, T. H. *Lichen biology* (Cambridge University Press, 1996).
2. Lutzoni, F. & Miadlikowska, J. Lichens. *Current Biology* **19**, R502–R503 (2009).
3. Hill, D. J. Asymmetric co-evolution in the lichen symbiosis caused by a limited capacity for adaptation in the photobiont. *The Botanical Review* **75**, 326–338 (2009).
4. Honegger, R. The lichen symbiosis—what is so spectacular about it? *The Lichenologist* **30**, 193–212 (1998).
5. Bronstein, J. L. Our current understanding of mutualism. *Quarterly Review of Biology* 31–51 (1994).
6. Dal Grande, F., Widmer, I., Wagner, H. & Scheidegger, C. Vertical and horizontal photobiont transmission within populations of a lichen symbiosis. *Molecular ecology* **21**, 3159–3172 (2012).
7. Sanders, W. B. & Lücking, R. Reproductive strategies, relichenization and thallus development observed in situ in leaf-dwelling lichen communities. *New Phytologist* **155**, 425–435 (2002).
8. Friedl, T. Thallus development and phycobionts of the parasitic lichen *Diploschistes muscorum*. *The Lichenologist* **19**, 183–191 (1987).
9. Dal Grande, F. *Phylogeny and co-phylogeography of a photobiont-mediated guild in the lichen family Lobariaceae*. Ph.D. thesis (2011).
10. Grube, M. & Spribille, T. Exploring symbiont management in lichens. *Molecular ecology* **21**, 3098–3099 (2012).
11. Yoshimura, I. Genus *Lobaria* of eastern asia. *Hattori Bot Lab J* (1971).
12. Škaloud, P., Friedl, T., Hallmann, C., Beck, A. & Dal Grande, F. Taxonomic revision and species delimitation of coccoid green algae currently assigned to the genus *Dictyochloropsis* (trebouxiophyceae, chlorophyta). *Journal of phycology* (2016).
13. Werth, S., Wagner, H. H., Holderegger, R., Kalwij, J. M. & Scheidegger, C. Effect of disturbances on the genetic diversity of an old-forest associated lichen. *Molecular Ecology* **15**, 911–921 (2006).
14. Walser, J.-C., Zoller, S., Büchler, U. & Scheidegger, C. Species-specific detection of lobaria pulmonaria (lichenized ascomycete) diaspores in litter samples trapped in snow cover. *Molecular Ecology* **10**, 2129–2138 (2001).
15. Werth, S. & Scheidegger, C. Congruent genetic structure in the lichen-forming fungus *Lobaria pulmonaria* and its green-algal photobiont. *Molecular Plant-Microbe Interactions* **25**, 220–230 (2012).
16. Rikkinen, J. Ecological and evolutionary role of photobiont-mediated guilds in lichens. *Symbiosis* **34**, 99–110 (2003).
17. Holland, J. H. Echoing emergence: Objectives, rough definitions, and speculations for echo-class models. In *Complexity*, 309–342 (Perseus Books, 1999).
18. Mitchell, M. *An introduction to genetic algorithms* (MIT press, 1998).
19. Newman, M. E. & Girvan, M. Finding and evaluating community structure in networks. *Physical review E* **69**, 026113 (2004).
20. Barber, M. J. Modularity and community detection in bipartite networks. *Physical Review E* **76**, 066102 (2007).
21. Larremore, D. B., Clauset, A. & Jacobs, A. Z. Efficiently inferring community structure in bipartite networks. *Physical Review E* **90**, 012805 (2014).

22. Flores, C. O., Poisot, T., Valverde, S. & Weitz, J. S. Bimat: a matlab package to facilitate the analysis of bipartite networks. *Methods in Ecology and Evolution* **7**, 127–132 (2016).
23. Poisot, T. An measure of network modularity a posteriori [version 2 (2013).
24. Atmar, W. & Patterson, B. D. The measure of order and disorder in the distribution of species in fragmented habitat. *Oecologia* **96**, 373–382 (1993).
25. Bascompte, J. & Jordano, P. The structure of plant-animal mutualistic networks. *Ecological networks: linking structure to dynamics in food webs*. Oxford University Press, Oxford, UK 143–159 (2006).
26. Bascompte, J., Jordano, P., Melián, C. J. & Olesen, J. M. The nested assembly of plant–animal mutualistic networks. *Proceedings of the National Academy of Sciences* **100**, 9383–9387 (2003).
27. Bascompte, J., Jordano, P. & Olesen, J. M. Asymmetric coevolutionary networks facilitate biodiversity maintenance. *Science* **312**, 431–433 (2006).
28. Rohr, R. P., Saavedra, S. & Bascompte, J. On the structural stability of mutualistic systems. *Science* **345**, 1253497 (2014).